

OPTICAL AND MAGNETIC RESPONSE OF PURE AND Cu-IONS SUBSTITUTED DYSPROSIUM OXIDE THIN FILMS FOR VARIOUS APPLICATIONS[†]

✉ **Muhammad Tauseef Qureshi***

Basic Science Department, College of Preparatory Year, University of Ha'il, 1560 Ha'il, Kingdom of Saudi Arabia

**Corresponding author e-mail: tauseefqureshi1981@gmail.com*

Received May 7, 2023; revised July 3, 2023; accepted July 4, 2023

Dysprosium oxide (Dy_2O_3) and Cu/Dy_2O_3 thin films of thickness 117.14 nm and 258.30 nm, respectively were successfully deposited via a well-known DC-magnetron sputtering technique. Field emission scanning electron microscopy clarifies the growth of uniform and fine granular particles on silicon substrate. The hexagonal closed pack structure for both the thin films has been observed by the x-ray diffraction analysis and it was observed that by inclusion of copper the HCP structure of thin film was retain with a slight shift in the main peak. The reduction from 3.9 eV to 3.8 eV in the energy band gap value was observed by incorporation of copper ions Dy_2O_3 thin films. The M-H loops obtained through Vibrating Sample Magnetometer (VSM) shows that Dy_2O_3 thin film behave ferromagnetically at low temperature with a saturation magnetization value of 2860 emu/cc and evolves through its phase transition temperatures and behave paramagnetically at room temperature. In Cu/Dy_2O_3 case, the diamagnetic response of Cu dominates and produces reverse hysteresis loop at both temperatures make it a suitable candidate for energy and memory storage devices applications.

Keywords: Magnetron sputtering; Dy_2O_3 ; Cu/Dy_2O_3 ; Thin films; Tauc plot; Magnetic properties; Hysteresis loop

PACS: 07.55.Jg, 61.10.Nz, 68.37.Hk, 74.25.Gz, 75.20.-g, 75.70.Ak, 81.20.-n

INTRODUCTION

During the last few years, several attempts have been made to improve the properties of rare-earth thin films by employing different methods. Successful approaches were to reduce their anisotropy different rare-earths were alloyed [1]; to include the tensile film stress [2], the preparation conditions were adjusted; to change the amorphous state of the films, small amount of Boron was added [3-4]. Among the rare-earth metals, Dy is considered as a possible solenoid pole piece material which is a suitable candidate for ultra-high moment applications at low temperatures [5-7]. The bulk Dy was considered as a pole material for field concentrators [8] and undulators [9], its tips for magnetic resonant force microscopy which can be used in pulsed-laser deposition, molecules beam epitaxy or plasma sputtering for its high yield and scalability [10]. Brilliant magneto-optical properties are resulted in the case of Copper (Cu) mixed with Manganese (Mn) for example, being Cu as optical and Mn as magnetic material [11]. The value of magnetic anisotropy of Dy is very large which when coupled with transition metals (Fe, Co, Ni, Cu) [12-14] and other ferromagnetic rare earths (Er, Ho, Gd) [15-20], much attention has been paid to DyFeCo [21], FeNdDyB [22] and FeDyTb alloys [23]. The slight structural changes incorporated because of guest molecules exchange, produce different dipole-dipole interactions which then effect the relaxation rate of incoherent quantum tunneling to acquire different effective relaxation barriers [24]. In this case, the structure of the near surface region of this phase becomes distorted; this leads to the nucleation of reverse magnetization domains to an experimentally observed decrease in H_{ci} [25].

Different properties of thin films are achieved by varying the production procedures as well as on the parameters of deposition, like deposition rate, temperature control, variation of substrate etc. In recent times, various physical and chemical deposition techniques are utilized for the processing of ZnO thin films, which includes but may not be restricted to, chemical vapor deposition (CVD), sputtering techniques, plasma enhanced CVD, sol-gel process and pulsed laser deposition (PLD) [26]. Among these growth techniques magnetron sputtering has a lot of advantages such as its low cost, low thermal budget, simplicity, non-toxic and for desired properties, its ability to produce high quality thin films [27]. Sezen et al studied the optical properties of Dy_2O_3 and recorded the band gap of 3.90 eV through ab-initio calculations to give way for the experimental growth of these thin film in combination with different metal content such Cu, Cr etc. [28]. The current study, we report the deposition of a high purity Dy_2O_3 and Cu/Dy_2O_3 thin films by DC magnetron sputtering on silicon substrate at room temperature. Further, the structural, morphology, optical and magnetic properties of these thin films Dy_2O_3 and Cu/Dy_2O_3 are investigated for energy and memory storage devices applications.

EXPERIMENTAL DETAILS

Sample Preparation

Dy_2O_3 and Cu/Dy_2O_3 thin films were fabricated via well-known sputtering technique using magnetron sputtering (DaON 1000 S) system contains three sputtering guns, one for Radio Frequency (RF) and two Direct Current (DC) supply [29-30]. The silicon substrate was used for the deposition of Dy and Cu and the temperature of it was kept up to 300°C. Initially, for achieving the clear and content free environment inside the chamber; high vacuum with base pressure of 5×10^{-6} Torr was achieved in 30 minutes before starting the deposition process. The Oxygen and Argon (70:30) flow were

[†] Cite as: M.T. Qureshi, East Eur. J. Phys. 3, 308 (2023), <https://doi.org/10.26565/2312-4334-2023-3-30>

© M.T. Qureshi, 2023

kept, but the flow rate was adjusted upto 5 mTorr. In the doping of Cu(10%) was controlled and calibrated by using STM (Sycon Thickness Monitor). The deposition of these films was carried out through DC sputtering keeping 300V and 100mA for Dy and 250V and 40mA for Cu respectively. Finally, thin films having thickness 117.14 nm & 258.30 nm for Dy₂O₃ and Cu/Dy₂O₃ respectively were collected after cooling the chamber to room temperature to avoid the deposited thin film from cracking down.

Sample Characterizations

The structure and crystallinity of the films were determined by an XRD (X'Pert) operating at 30 kV and 10 mA using Cu K_{α1} radiation (1.54 Å). The measurement was conducted at room temperature with $2\theta = 20^{\circ}$ - 70° incident angles. For morphological study of these thin films FESEM (FEI Nova 450) was used. The operating power of the FEI Nova 450 was 10 kV and 50kV respectively. The microscope was in the secondary electron mode at a working distance of 5.1 mm with lens detector. EDX spectrometry (Oxford Instruments Inca X-Act) built in with FEI Nova 450, was used for qualitative and quantitative compositions analysis of elements. Spectroscopic Ellipsometry (Alpha-SE Ellipsometer, J. A. Woollam) was used to get the thickness of thin films and absorption coefficient of thin films. Hysteresis loop for magnetization of the Dy₂O₃ and Cu/Dy₂O₃ thin films was obtained using a VSM (with low temperature 5K and at room temperature 300K) using Cryogen free measuring system (Cryogen Limited UK).

RESULTS AND DISCUSSION

Structural Analysis

Figure 1 shows crystallographic results i.e., XRD peaks and their miller indices of Dy₂O₃ and 10%-Cu substituted Dy₂O₃ thin films. For Dy₂O₃, two peaks are observed, one at 28.23° with miller indices (100) and other at 32.40° having Miller indices (101) as shown by Figure 1(a).

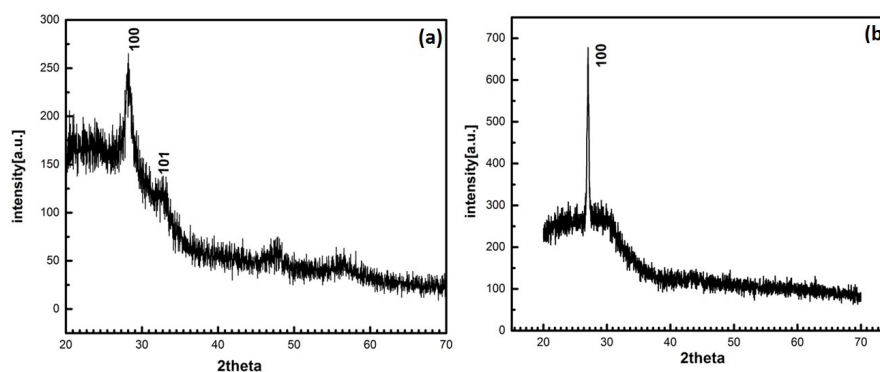


Figure 1. XRD pattern of (a) Dy₂O₃ and (b) Cu/Dy₂O₃ thin films

The comparison of Dy₂O₃ XRD data with the reference code 01-089-2926, confirm the hexagonal closed pack (hcp) structure and having space group P63/mmc and space number of 194. When 10%-Cu is co-deposited with Dy for the alloy thin film, only a single prominent, sharp peak has been observed, as in Figure 1(b). This peak is associated to Dy₂O₃, since having miller indices of (100) for 2θ value of 27.03° .

It can be found that the presence of Cu has slightly adjusted the (100) peak to new 2θ value and no peak for Cu has been observed in the Cu/Dy₂O₃ thin film. It has been found for the case of Cu mixed ZnO thin films [31, 32] that the introduction of Cu adjusts the main peak of ZnO (002) to new values of 2θ and with no Cu peak. They have suggested that there is strong c-orientation preference with normal to the substrate and Cu atoms exist only on the interstitial sites. The same can be attributed in current scenario where Dy₂O₃ having close packing structure with maximum packing density does not allow Cu atoms to change/modify the base Dy₂O₃ structure, rather be present at the interstitial sites thus increasing the overall energy. Recalling the Cu standard pattern having reference No. 04-0836, there are three prominent peaks for copper, each at 43.30° , 50.43° & 74.13° 2θ values, but Figure 1(b) announces no peak (even smaller one) at the above-mentioned values for Cu.

Morphological studies and elemental analysis

FESEM micrographs of Dy₂O₃ and Cu/Dy₂O₃ thin films are shown in figure 2(a-d) (where a, b represents the Dy₂O₃ micrographs, and c, d show Cu/ Dy₂O₃ images). It is clear from the micrographs of these thin films that growth of smooth and uniformly dispersed particles along with small grains on the silicon substrate, which can be due to the fact that both Dy₂O₃ and Cu/Dy₂O₃ are deposited simultaneously. Moreover, inclusion of Cu as dopant or co-dopant normally smoothens the ZnO thin film structure as can be found in many semiconductors' technologies-based materials [33].

The EDX spectra of pure and Cu substituted thin films were acquired by using 20 kV electron beam-energy are shown in Figure 3. The Cu, Dy and O intensities peaks in both thin films confirmed its high-purity and the presence of these acquired elements with their stoichiometric ratio. The table within figure 3 shows the wt% of each constituent elements with their stoichiometric-formulation.

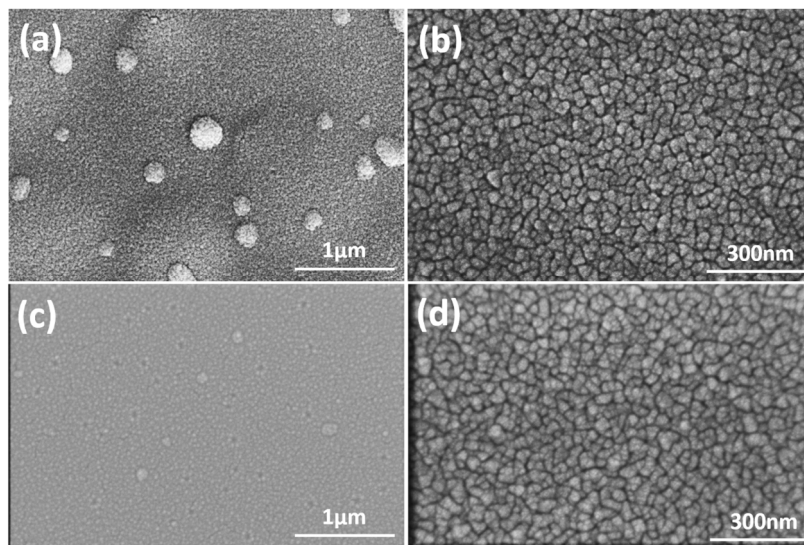


Figure 2. FESEM micrographs at lower and higher magnification (a, b) Dy₂O₃, and (c, d) Cu/ Dy₂O₃ thin film

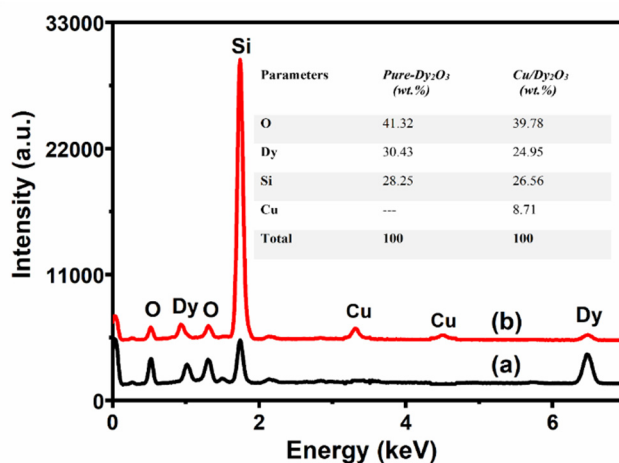


Figure 3: EDS spectra of thin films with their table of elements compositions wt.% where (a) shows Dy₂O₃ and (b) 10%-Cu doped Dy₂O₃ thin films compositions

Optical Studies

The absorption coefficient energy band gap curve obtained through ellipsometry and Tauc and Davis's plot respectively are shown in Figure 4.

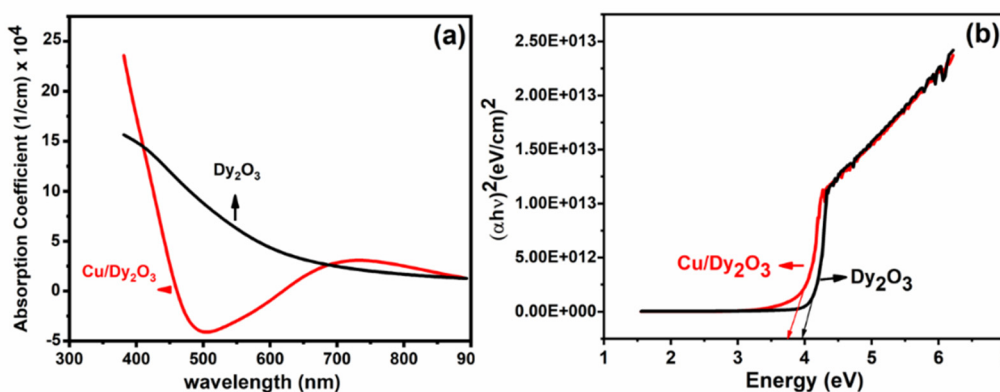


Figure 4: Optical properties measurement through ellipsometry (a) Absorption coefficient and (b) Energy band gap values for both thin films as plotted by the Tauc plot

The absorption coefficient value high at lower wavelength shows high value, but as the wavelength shifted towards the visible region that it decreases for both samples and finally a slight increase at the elevated wavelength as shown in

Figure 4(a). Which shows that these thin films are good observers at lower wavelength. Figure 4(b) represents the energy band gap value 3.8 eV for Dy_2O_3 and 3.9 eV for Cu/Dy_2O_3 thin films obtained from Tauc and Davis's plot in which the photon energy and absorption coefficient can be related in the absorbance region in a relation expressed as:

$$ah\nu = A(h\nu - E_g)^n \quad (1)$$

where " α " is the absorption coefficient, " $h\nu$ " is photon energy, " A " is proportionality constant, " E_g " is optical band gap, " n " is an integer equal to 2 for an indirect and 1/2 for direct band gap in the above relation [34]. For the value of $n=2$ for Dy_2O_3 and Cu/Dy_2O_3 thin films, it states that an indirect band gap obtained for these structures. Similarly, energy band of Dy_2O_3 confirms the fact that valance shell electrons have the ability of absorbing energy, whereas value for second thin film Cu/Dy_2O_3 decrease which further enhances the chance for such materials to be used in electronic applications.

Magnetic Properties Studies

Figure 5 represents the magnetic hysteresis loops of Dy_2O_3 and Cu/Dy_2O_3 thin films at room temperature (300K) and low temperature 5K as presented in figure 5.

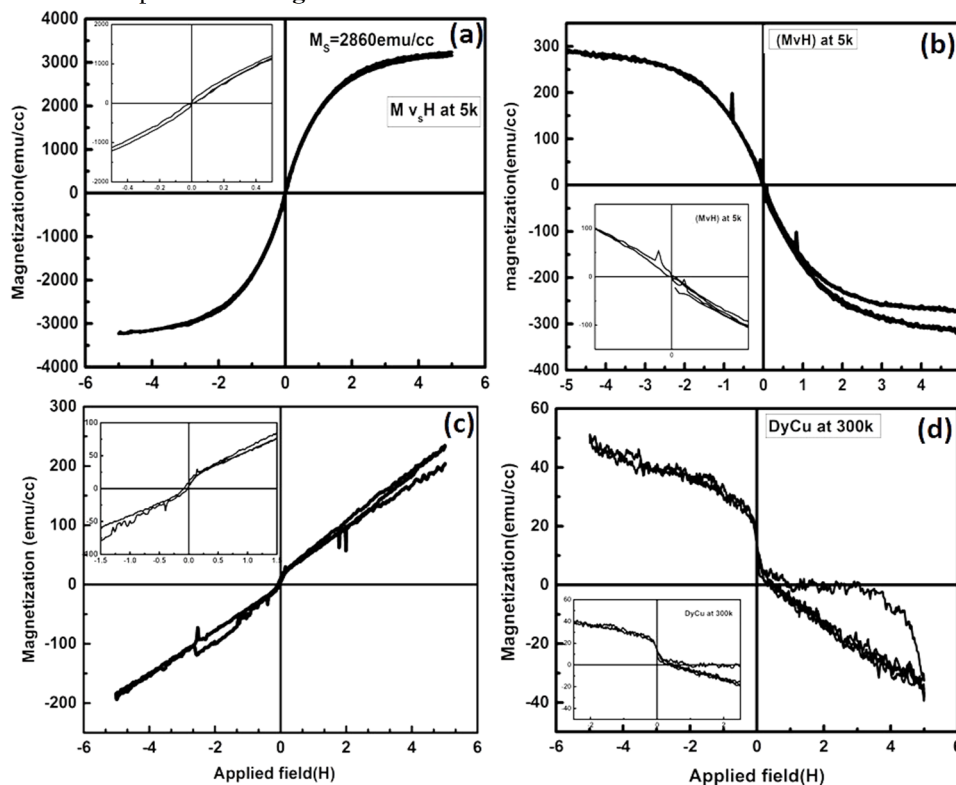


Figure 5. Shows M-H curves, here (a) presents Dy_2O_3 at 5k, (b) Cu/Dy_2O_3 at 300k, (c) Dy_2O_3 at 5k and (d) Cu/Dy_2O_3 at 300k, respectively

The ferromagnetic order in case of Dy_2O_3 at 5 K has been observed, since its behavior evaluates into anti-ferromagnetic ordering at above 85 K and further to paramagnetic nature at and above 179 K. The M_s value obtained for Dy_2O_3 thin film at low temperature is 2860 emu/cc. The inset of Figure 5(a) shows that the magnetization lines pass through the origin, announcing no remanent magnetization [35], a response typically related to pure ferromagnetic materials. Moreover, when magnetization for Dy_2O_3 thin film is measured at room temperature (Figure 5(c)), a paramagnetic type of behavior is observed, with much reduced saturation magnetization value and obviously no remanent magnetization as in the inset of this graph (Figure 5(c)).

A completely different response of the Cu/Dy_2O_3 thin film has been observed both at low and room temperature, with production of reverse hysteresis loop due to inclusion of Cu with Dy. The energy difference between the lowest doubly degenerate sublevels (formally corresponding to large J_z values of $\pm 11/2$ or $\pm 13/2$ for dysprosium) seems to be affected by the degree of longitudinal compression or elongation [36-37]. This behavior of the Cu/Dy_2O_3 thin film can be due to the effect of Cu diamagnetic nature, which drives Dy to behave diamagnetically and pronounces a small magnetization value. The difference above may be linked with the different local symmetry and the bond distances result in different ligand fields [38]. The behavior of Cu/Dy_2O_3 thin film has also the support of XRD data as presented above, with Cu atoms present at the interstitial sites, not affecting the structure, rather other physical properties of the thin film. For the case of Dy_2O_3 Figure 5(c) it is clear that dysprosium thin film transforms to paramagnetic nature with an improper saturation of the particles and a much-reduced saturation magnetization value. These results can be used for the tuning of magnetic properties of Dy based thin films for technological applications [15-20].

CONCLUSION

Thin films of Dy₂O₃ and Cu/Dy₂O₃ of thickness 17.14 nm and 258.30 nm respectively were prepared successfully by the magnetron sputtering method. It is suggested that Cu elements residing at the interstitial sites, not affecting the structure of the alloyed thin film, as confirmed by the XRD results but modify the other physical properties. Smooth behavior of the thin films is obtained by the FESEM micrographs along with no impurity shown by the elemental analysis through EDX. Further, by addition of Cu reveals a change in the optical properties, as well as diamagnetic response of the Cu compels Dy to produce negative hysteresis effect (by VSM) can be used for such material-based storage application.

Acknowledgment

The author gratefully acknowledges Dr. Faman Ullah for assisting in getting the results.

ORCID

© Muhammad Tauseef Qureshi, <https://orcid.org/0000-0001-7388-8512>

REFERENCES

- [1] F. Schatz, M. Hirscher, G. Flik, and H. Kronmüller, *Physica Status Solidi*, **137**(1), 197 (1993). <https://doi.org/10.1002/pssa.2211370117>
- [2] G. Flik, M. Schnell, F. Schatz, and M.B. Hirscher, in: *Proc. Actuator 94*, (Bremen, Germany, 1994), p. 232.
- [3] J.Y. Kim, *J. Appl. Phys.* **74**, 2701 (1993). <https://doi.org/10.1063/1.354664>
- [4] R. Jain, V. Luthra, and S. Gokhale, *J. Mag. and Mag. Mater.* **456**, 179 (2018). <https://doi.org/10.1016/j.jmmm.2018.02.029>
- [5] H. Fernández-Morán, *Physics*, **53**, 445 (1965). <https://doi.org/10.1073/pnas.53.2.445>
- [6] A. Paulson, N.M. Sabeer, and P.P. Pradyumnan, *Mater. Sci. & Engi. B*, **262**, 114745 (2020). <https://doi.org/10.1016/j.mseb.2020.114745>
- [7] A. Bulatov, S. Goridov, M. Tikhonovskij, and S. Novikov, *IEEE Trans. Mag.* **28**, 509 (1992). <https://doi.org/10.1109/20.119923>
- [8] R. Agustsson, P. Frigola, A. Murokh, O. Chubar, and V. Solovyov, in: *Proceedings of 2011 Particle Accelerator Conference*, (New York, USA, 2011), pp. 1256-1258.
- [9] R. Agustsson, P. Frigola, A. Murokh, and V. Solovyov, in: *Proceedings of PAC09*, (Vancouver, Canada, 2009), WE5RFP077.
- [10] Z.S. Shan, and D.J. Sellmyer, *J. Appl. Phys.* **64**, 5745 (1988). <https://doi.org/10.1063/1.342245>
- [11] N.D. Subramanian, J. Moreno, J.J. Spivey, and C.S. Kumar, *J. Phys. Chem. C*, **115**, 14500 (2011). <https://doi.org/10.1021/jp202215k>
- [12] Z.S. Shan, S. Nafis, K.D. Aylesworth, and D.J. Sellmyer, *J. Appl. Phys.* **63**, 3218 (1988).
- [13] A.V. Trukhanov, K.A. Astapovich, V.A. Turchenko, M.A. Almessiere, Y. Slimani, A. Baykal, A.S.B. Sombra, *et al.*, *J. Alloys Compounds*, **841**, 155667 (2020). <https://doi.org/10.1016/j.jallcom.2020.155667>
- [14] K. Dumesnil, C. Dufour, P. Mangin, G. Marchal, and H. Hennion, *Phys. Rev. B*, **54**, 6407 (1996). <https://doi.org/10.1103/PhysRevB.54.6407>
- [15] K. Dumesnil, C. Dufour, P. Mangin, G. Marchal, and H. Hennion, *Europhys. Let.* **31**(1), 43 (1995). <https://doi.org/10.1209/0295-5075/31/1/008>
- [16] M. Elisa, R. Stefan, I.C. Vasiliu, M.I. Rusu, B.A. Sava, L. Boroica, M. Sofronie, *et al.*, *J. Non-cryst. Solids*, **521**, 119545 (2019). <https://doi.org/10.1016/j.jnoncrysol.2019.119545>
- [17] A.M. Henaish, O.M. Hemeda, E.A. Arrasheed, R.M. Shalaby, A.R. Ghazy, I.A. Weinstein, M.A. Darwish, *et al.*, *J. Compos. Sci.* **7**, 61 (2023). <https://doi.org/10.3390/jcs7020061>
- [18] G. Ganesh, A. Sandeep, G. Chanti, R.S. Bose, M.S. Kumar, K.P. Kumari, T. Shekharam, *et al.*, *Phys. Stat. solidi (a)*, **220**(9), 2200864 (2023). <https://doi.org/10.1002/pssa.202200864>
- [19] G. Hussain, I. Ahmed, A.U. Rehman, M.U. Subhani, N. Morley, M. Akhtar, M.I. Arshad and H. Anwar, *J. Alloys & Comp.* **919**, 165743 (2022). <https://doi.org/10.1016/j.jallcom.2022.165743>
- [20] T.H. Wu, J.C. Wu, B.M. Chen, and H.P.D. Shieh, *J. Mag. Mag. Mater.* **202**, 62 (1999). [https://doi.org/10.1016/S0304-8853\(99\)00140-7](https://doi.org/10.1016/S0304-8853(99)00140-7)
- [21] S. Sugimoto, *J. Phys. D: Appl. Phys.* **44**, 064001 (2011). <https://doi.org/10.1088/0022-3727/44/6/064001>
- [22] C.V. Mohan, and H. Kronmüller, *J. Alloys Compounds*, **267**, L9 (1998). [https://doi.org/10.1016/S0925-8388\(97\)00524-0](https://doi.org/10.1016/S0925-8388(97)00524-0)
- [23] A.M. Tishin, and Y.I. Spichkin, *The Magnetocaloric Effect and its Applications*, (IOP Publishing Ltd., London, 2003).
- [24] S. Zhang, K. Hongshan, S. Lin, L. Xin, S. Quan, X. Gang, W. Qing, *et al.*, *Inorganic Chemistry*, **55**, 3865 (2016). <https://doi.org/10.1021/acs.inorgchem.5b02971>
- [25] V.P. Piskorskii, G.S. Burkhanov, O.G. Ospennikova, R.A. Valeev, I.S. Tereshina, and E.A. Davydova, *Russian Metallurgy*, **5**, 442 (2010). <https://doi.org/10.1134/S0036029510050150>
- [26] Y.S. Kim, H.J. Park, S.C. Mun, E. Jumaev, S.H. Hong, G. Song, J.T. Kim, *et al.*, *Alloys & Comp.* **797**, 834 (2019). <https://doi.org/10.1016/j.jallcom.2019.05.043>
- [27] J. Kar, S. Kim, B. Shin, and J. Myong, *Solid-State Electronics*, **54**, 1447 (2010). <https://doi.org/10.1016/j.sse.2010.07.002>
- [28] S. Horoz, S. Simsek, S. Palaz, A.M. Mamedov, E. Ozbay, *International Journal of Scientific and Technological Research*, **1**, 36 (2015). <https://www.iiste.org/Journals/index.php/JSTR/article/view/23009/23526>
- [29] S.M. Ramay, A. Mahmood, H.M. Ghaitan, N.S. Al-Zayed, A. Aslam, A. Murtaza, N. Ahmad, *et al.*, *J. Rare Earths*, **37**, 989 (2019). <https://doi.org/10.1016/j.jre.2018.12.002>
- [30] P. Salunkhe, M.A.V. Ali, and D. Kekuda, *Mater. Res. Exp.* **7**, 016427 (2020). <https://doi.org/10.1088/2053-1591/ab69c5>
- [31] P.S. Shewale, V.B. Patil, S.W. Shin, J.H. Kim, and M.D. Uplane, *Sens. Actuators B: Chem.* **186**, 226 (2013). <https://doi.org/10.1016/j.snb.2013.05.073>
- [32] X.B. Wang, D.M. Li, F. Zeng, and F. Pan, *J. Phys. D: Appl. Phys.* **38**, 4104 (2005). <https://doi.org/10.1088/0022-3727/38/22/014>

- [33] H. Gong, J.Q. Hua, J.H. Wang, C.H. Onga, F.R. Zhub, Sens. Actuators B: Chem. **115**, 247 (2006). <https://doi.org/10.1016/j.snb.2005.09.008>
- [34] F.Y. Lo, Y.C. Ting, K.C. Chou, T.C. Hsieh, C.W. Ye, Y.Y. Hsu, M.Y. Chern, and H.L. Liu, J. Appl. Phys. **117**, 213911 (2015). <https://doi.org/10.1063/1.4921979>
- [35] S.E. Harrison, L.J. Collins-McIntyre, S.L. Zhang, A.A. Baker, A.I. Figueroa, A.J. Kellock, A. Pushp, J. Phys. Condens. Matter. **27**, 245602 (2015). <https://doi.org/10.1088/0953-8984/27/24/245602>
- [36] K. Niira, Phys. Rev. **117**, 129 (1960). <https://doi.org/10.1103/PhysRev.117.129>
- [37] M. Morishita, T. Abe, H. Yamamoto, A. Nozaki, and S. Kimura, Thermoch. Act, **721**, 179410 (2023). <https://doi.org/10.1016/j.tca.2022.179410>
- [38] L.I. Naumova, M.A. Milyaev, R.S. Zavornitsyn, T.P. Krinitsina, V.V. Proglyado, and V.V. Ustinov, Curr. Appl. Phys. **19**, 1252 (2019). <https://doi.org/10.1016/j.cap.2019.08.012>
- [39] K.P. Belov, R.Z. Levitin, and S.A. Nikitin, Soviet Physics Uspekhi, **7**, 179 (1964). <https://doi.org/10.1070/PU1964v007n02ABEH003660>

ОПТИЧНИЙ ТА МАГНІТНИЙ ВІДГУК ЧИСТИХ ТА НАСИЧЕНИХ ІОНАМИ Cu ТОНКИХ ПЛІВОК ОКСИДУ ДИСПРОЗИЮ, ДЛЯ РІЗНИХ ЗАСТОСУВАНЬ

Мухаммад Таусеф Куреші

*Факультет фундаментальних наук, Коледж підготовчого року, Університет Хайль,
Хайль, Королівство Саудівська Аравія*

Тонкі плівки оксиду диспрозю (Dy_2O_3) і Cu/Dy_2O_3 товщиною 117,14 нм і 258,30 нм відповідно були успішно нанесені за допомогою добре відомого методу магнетронного напилення на постійному струмі. Автоемісійна скануюча електронна мікроскопія показала зростання однорідних і дрібних гранульованих частинок на кремнієвій підкладці. Гексагональна закрита структура пакування для обох тонких плівок спостерігалася за допомогою рентгенівського дифракційного аналізу, і було помічено, що завдяки включенню міді НСР-структура тонкої плівки зберігалася з невеликим зсувом головного піку. Зменшення ширини забороненої зони від 3,9 еВ до 3,8 еВ спостерігалася шляхом включення тонких плівок іонів міді Dy_2O_3 . Петлі М-Н, отримані за допомогою вібраційного магнітометра (VSM), показують, що тонка плівка Dy_2O_3 поводить себе феромагнітно при низькій температурі зі значенням намагніченості насичення 2860 етл/сс і розвивається через температури фазового переходу та поводить себе парамагнітно при кімнатній температурі. У випадку Cu/Dy_2O_3 діамагнітний відгук Cu домінує та створює петлю зворотного гістерезису при обох температурах, що робить його придатним кандидатом для додатків пристроїв зберігання енергії та пам'яті.

Ключові слова: магнетронне розпилення; тонкі плівки; Dy_2O_3 ; Cu/Dy_2O_3 ; графік Таука; магнітні властивості; петля гістерезису